Materials and Structures

Improved assessment of Fibre Content and Orientation with Inductive Method in SFRC

--Manuscript Draft--

Manuscript Number:	MAAS-D-13-00598
Full Title:	Improved assessment of Fibre Content and Orientation with Inductive Method in SFRC
Article Type:	Original Research
Keywords:	SFRC; inductive method; fibre content; orientation number; quality control
Corresponding Author:	Sergio Henrique Pialarissi Cavalaro, Ph.D. Universidad Politécnica de Cataluña Barcelona, Catalunya SPAIN
Corresponding Author Secondary Information:	
Corresponding Author's Institution:	Universidad Politécnica de Cataluña
Corresponding Author's Secondary Institution:	
First Author:	Sergio Henrique Pialarissi Cavalaro, Ph.D.
First Author Secondary Information:	
Order of Authors:	Sergio Henrique Pialarissi Cavalaro, Ph.D.
	Rubén López, Civil Engineer
	Josep María Torrents, Ph.D.
	Antonio Aguado, Ph.D.
Order of Authors Secondary Information:	
Abstract:	The inductive method is a robust and simple non-destructive test to assess the content and the distribution of the fibres in SFRC. Despite the advantages in comparison with other methods, further studies are still needed to define the accuracy, the theoretical basis and the equations for the conversion of the inductance into fibre content and distribution. In fact, although the test provides an indirect estimation of the fibre distribution, currently no equation exists for the assessment of the orientation number, which is a valuable parameter for the design of structures. The objective of the present paper is to address this issue. Initially, the theoretical basis for the calculation of the fibre content is provided. Then, alternative equations are deducted for the fibre contribution and for the orientation number. Different experimental programs and finite element numerical simulations are conducted to evaluate the accuracy of the method and to validate the proposals. The results indicate that the equations currently used may lead to errors of up to 24%. Instead, the formulation proposed here show errors far below 2.6%, allowing the prediction of the orientation number in all directions with a high accuracy. This opens up a new field of application for the test and represents an advance towards the characterization and the quality control of SFRC.

Improved assessment of Fibre Content and Orientation with Inductive Method in SFRC

Sergio H. P. CAVALARO [1*], Rubén LÓPEZ [1], Josep María TORRENTS [2], Antonio AGUADO [1]

[1] Departamento de Ingeniería de la Construcción, ETSECCPB, Universidad Politécnica de Cataluña, BarcelonaTech, Calle Jordi Gironal 1-3, 08034, Barcelona, Spain

[2] Departamento de Ingeniería Electrónica, EEL, Universidad Politécnica de Cataluña, BarcelonaTech, Calle Jordi Gironal 1-3, 08034, Barcelona, Spain

* Corresponding author: Despacho 106, Edificio B1, Campus Nord, Departamento de Ingeniería de la Construcción, ETSECCPB, Universidad Politécnica de Cataluña, BarcelonaTech, Calle Jordi Gironal 1-3, 08034, Barcelona, Spain, email sergio.pialarissi@upc.edu, Phone (+34) 934054247, Fax (+34) 934054135

Abstract

The inductive method is a robust and simple non-destructive test to assess the content and the distribution of the fibres in SFRC. Despite the advantages in comparison with other methods, further studies are still needed to define the accuracy, the theoretical basis and the equations for the conversion of the inductance into fibre content and distribution. In fact, although the test provides an indirect estimation of the fibre distribution, currently no equation exists for the assessment of the orientation number, which is a valuable parameter for the design of structures. The objective of the present paper is to address this issue. Initially, the theoretical basis for the calculation of the fibre content is provided. Then, alternative equations are deducted for the fibre contribution and for the orientation number. Different experimental programs and finite element numerical simulations are conducted to evaluate the accuracy of the method and to validate the proposals. The results indicate that the equations currently used may lead to errors of up to 24%. Instead, the formulation proposed here show errors far below 2.6%, allowing the prediction of the orientation number in all directions with a high accuracy. This opens up a new field of application for the test and represents an advance towards the characterization and the quality control of SFRC.

Keywords: *SFRC; inductive method; fibre content; orientation number; quality control*

1. Introduction

The mechanical response of steel fibre reinforced concrete (SFRC) is dependent of the fibre content and orientation within the concrete matrix [1-3]. The content affects the probabilistic of finding a fibre that cross the cracked section [4]. Moreover, the orientation assumed by the fibres determines their average angle with the cracked plane, which is related with their bridging capacity [5-8]. Due to the high repercussion of the subject [9 - 13], the quality control of SFRC in the worksite usually includes tests to assess the content and the distribution profile of fibres.

The manual determination is the most common test that may be performed with fresh and hardened representative samples. In the first case, the fibres are washed out from the fresh material and then weighted to determine the content. In the second case, after the samples are crushed, the fibres are separated and weighted. Both procedures are detailed in the standard EN 14721.The main advantage of the manual tests is the straightforward procedure that uses equipment available in most worksites. However, the determination is restricted to the fibre content while the evaluation of the orientation is not possible. In addition to that, the long time needed to conduct each test and the high amount of waste generate limit the number of assessments conducted per batch. This hinders the representativeness of the results given the high scatter of SFRC, thus leading to problems in the quality control.

Advanced techniques based on the image analysis were successfully used in studies from the literature. In general lines, sectional images of the samples at different points are taken through X-ray [14-16] or tomography [17, 18]. Then, algorithms for the computerized processing of the images are used to determine a 3D distribution profile of the fibres [19]. Although these techniques allow a detailed discretization of the sample, they usually require a long time of preparation or execution combined with expensive large-scale equipment that is not available in the worksite.

As a more economic and practical alternative for the quality control, several indirect methods were already proposed to assess properties that later may be correlated with the fibres distribution. Examples are the ones based on impedance spectroscopy [20, 21], microwaves [22, 23], electric resistance [24, 25] or inductance [26 - 28]. Despite the advantages in terms of the cost of equipment and time dedicated to each test, some of them present limitations. For instance, the results obtained with methods based on electroscopy and electric resistance vary with the age of concrete whereas the methods based on the impedance and the microwaves only allow a superficial characterization of the SFRC.

In this context, the inductive method proposed by Torrents et al. [28] is a robust alternative since the results obtained are not affected by the age of concrete and bigger volumes of material may be assessed. Despite the advantages mentioned, further studies are still needed to define the accuracy, the theoretical basis of the test and the equations for the conversion of the inductance measurements into fibre content and distribution. Another drawback of the method is that no equation exists for the estimation of the orientation number, which is a valuable parameter for the design of structures.

The objective of the present paper is to address this issue, proposing and validating the equations to quantify the fibre distribution in SFRC. Initially, a brief description of the method and of the equations currently used is presented along with the theoretical deduction of the alternative formulation proposed. Then, different experimental programs and finite element numerical simulations are conducted to evaluate the accuracy of the method as well as to validate the formulations obtained. The conclusions derived from this study represent an advance towards the characterization of SFRC. Additionally, they contribute to the development of an improved quality control system that may be easily implemented in the worksite with faster measurements in a bigger number of specimens and more reliable results.

2. Description of the inductive method

The method proposed by Torrents et al. [28] consists of measuring the inductance change produced when a magnetic field is applied to a SFRC sample. As shown in Fig. 1.a, the equipment is composed by an impedance analyser that generates an electric current flow in a discontinuous coil with a square cross section. The current flow produces a magnetic field inside the coil. When the sample is introduced in the coil, the ferromagnetic nature of the fibres increases the magnetic permeability of the medium and, consequently, the inductance variation is measured with the analyser.

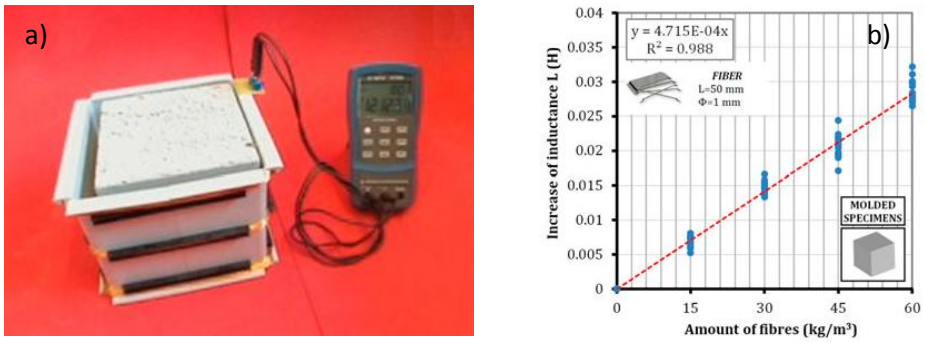

Fig. 1.- Inductive method proposed by Torrents et al. [28] (a) and typical relation between inductance change and fibre content (b)

The test is designed for 15 cm cubic specimens, which may be later used for mechanical characterization through the Barcelona test (UNE 83515) [29]. The inductance of each sample is measured for the main directions perpendicular to the faces of the cubic specimen. This yields the measurements ΔL_x, ΔL_y and ΔL_z for the axis X, Y and Z, respectively. Further information about the method may be found in [28].

For very small amounts of fibre, Torrents et al. [28] demonstrates that the inductance change in a certain direction should be proportional to the content. However, this is true only if the orientation of fibres is maintained constant. In fact, the correlations between the inductance change in a certain direction and the fibre content is not acceptable in case the test is performed with concretes with very different orientation profiles, such as vibrocompactated and self-compacting.

Experimental results show that the summed inductance for the three axes (ΔL) holds a linear relation with the fibre content (see Fig. 1.b), with a proportionality constant ω. This relation is mantained regardless of the distribution of fibres in the specimen. Consequently, if the calibration curve is known in advance for the type of fibre, the estimation of the content (C_f) may be performed with an accuracy of 5% through a simple linear conversion shown in Eq. 1 [28]. However, no theoretical basis is presented to justify why the summed inductance for the three axes should be used nor the accuracy of the method is extensively studied.

$$C_f = \omega \cdot \sum_{i=x,y,z} \Delta L_i = \omega \cdot \Delta H \qquad \textit{Eq. 1}$$

The same authors suggest that a fair estimation of the fibre orientation may also be obtained with the inductance measurements by using the relative contribution of fibre in a certain direction (C_i) estimated through Eq. 2. Despite the reasonable results obtained with this equation, theoretical foundation or validations are not provided to support its use.

$$C_i = \frac{\Delta L_i}{\Delta L} \qquad \textit{Eq. 2}$$

3. Analytical deductions

3.1. Theoretical basis

To deduct the theoretical basis and the formulations for the fibres distribution, some assumptions are made. It is considered that the magnetic field generated inside the coil is practically uniform and that the interaction between fibres may be ignored. Furthermore, since the magnetic permeability of steel is several orders of magnitudes higher than that of concrete, the contribution of the latter is disregarded to simplify the deduction.

The conventional approach would be to use the Maxwell's equations to account for the increase of the magnetic permeability produced inside the coil due to the inclusion of fibres and the consequent inductance change. However, this would lead to a very complex and lengthy deduction. Rather than that, an analogy with the mutual inductance is used, as in other widely accepted deductions from the electromagnetism theory.

It is known that a polarization of each fibre occurs when they are subjected to a magnetic field. This may be represented as if each fibre was an equivalent solenoid that might interact with the coil producing a mutual inductance or an inductance change (ΔL_i). According with the electromagnetic theory, the mutual inductance produced between a solenoid and a coil that receives an electric current (I) may be estimated through Eq. 3. In this equation, Φ_i represents the magnetic flux generated by the coil that goes through the solenoid.

$$\Delta L_i = \frac{\emptyset_i}{I} \qquad \textit{Eq. 3}$$

Notice that the electric current (I) is maintained constant during the test. Consequently, ΔL_i may be estimated if Φ_i is known. Suppose now a single fibre whose length forms an angle α_i with the magnetic field B inside the coil, as shown in Fig. 2.a.

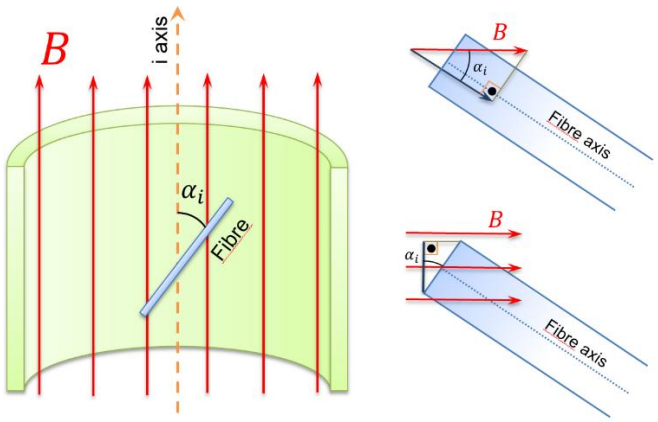

Fig. 2. Single fibre inside a coil (a) and decomposition of the magnetic flux through the fibre (b and c)

In order to estimate the magnetic flux along the length of the fibre ($\emptyset_{\parallel}$), the magnetic field flux density (B) must be decomposed twice. The first decomposition (see Fig. 2.b) accounts for the increase of the area that is crossed by the flux. The second decomposition accounts for the modification of the direction shown in Fig. 2.c. In both cases the cosine of α is multiplied by B, yielding Eq. 4 that also includes the constant k' to consider the properties of the material of the fibre.

$$\emptyset_{\parallel} = k' \cdot B \cdot cos^2\alpha_i \qquad Eq.\ 4$$

Even though the biggest change in the inductance is produced by the equivalent solenoid along the length of the fibre, a second equivalent solenoid could be observed along the width. The latter would induce smaller ΔL due to a shape effect represented by the coefficient γ. Furthermore, the equivalent solenoid perpendicular to the length of the fibre would form an angle that is the trigonometric complement of α_i. Similarly to what was done in Eq. 4, these considerations allow the deduction of Eq. 5 for the magnetic flux in the direction perpendicular to the length of the fibre ($\emptyset_{\perp}$).

$$\emptyset_{\perp} = \gamma \cdot k' \cdot B \cdot sin^2\alpha_i \qquad Eq.\ 5$$

Combining Eq. 3 to 5 gives Eq. 6. Alternatively, a simple trigonometric equivalence may be used to derive Eq. 7 for the change of inductance in the coil due to the inclusion of a single fibre.

$$\Delta L_i = \frac{\emptyset_{\parallel} + \emptyset_{\perp}}{I} = \frac{k' \cdot B}{I} \cdot (cos^2\alpha_i + \gamma \cdot sin^2\alpha_i) \qquad Eq.\ 6$$

$$\Delta L_i = k \cdot [cos^2\alpha_i + \gamma \cdot (1 - cos^2\alpha_i)] \qquad Eq.\ 7$$

If the measurements are taken in the three main Cartesian axes, the summed result would be given by Eq. 8. Notice that the angles α_x, α_y and α_z are complementary in space. This means that the sum of the square of the cosine of the angles must equal 1. Consequently, Eq. 8 may be rewritten as shown in Eq. 9.

$$\Delta L = k \cdot \sum_{i=x,y,z} [cos^2\alpha_i + \gamma \cdot (1 - cos^2\alpha_i)] \qquad \textit{Eq. 8}$$

$$\Delta L = k \cdot (1 + 2 \cdot \gamma) \qquad \textit{Eq. 9}$$

The latter indicates that the summed measurement of the inductive method for the three axes for a single fibre do not depend on its position or on its direction. In other words, the results will remain the same regardless on how the inclusion in made. This combined with the fact that the interaction between fibres is depreciable in comparison with the interaction with the coil for the contents commonly used in FRC, allows the deduction of Eq. 10 for the case with several inclusions. In such equation n represents the number of fibres present, which may be rewritten as a function of the content of fibres in weight per unit of volume (C_f), the density of steel (ρ), the volume of the specimen (V), the diameter (d) and the aspect ratio (λ) of the fibre.

$$\Delta L = k \cdot (1 + 2 \cdot \gamma) \cdot n = k \cdot (1 + 2 \cdot \gamma) \cdot \frac{4 \cdot C_f \cdot \lambda \cdot V}{\pi \cdot \rho \cdot d^3} \qquad \textit{Eq. 10}$$

Isolating C_f in Eq. 10 gives Eq. 11. Notice that the term multiplying the result of the inductive method (ΔL) is composed solely by constants that depend on the characteristics of the fibre and of the coil. This indicates that a linear relation should exist between ΔL and C_f, thus confirming the experimental observations. The proportionality constant ω between both parameters included in Eq. 1 may be estimated through Eq. 12.

$$C_f = \frac{\pi \cdot \rho \cdot d^3}{4 \cdot \lambda \cdot k \cdot V \cdot (1 + 2 \cdot \gamma)} \cdot \Delta L \qquad \textit{Eq. 11}$$

$$\beta = \frac{\pi \cdot \rho \cdot d^3}{4 \cdot \lambda \cdot k \cdot V \cdot (1 + 2 \cdot \gamma)} \qquad \textit{Eq. 12}$$

3.2. Orientation number and contribution of fibres

Once the theoretical basis is established, the formulations to predict the orientation of fibres may be deducted. As in many other studies from the literature, the parameter used to assess the contribution of the fibre in a certain direction is the average orientation number (η_i), extensively described in [30 - 33]. Such number is given by the average of the cosine of the

angle formed between the fibres that compose the material and a line parallel to the direction in question. Therefore, the first step to predict the orientation number is to estimate the average cosine of the angles from the result of the inductive method. A fair approximation may be obtained by rearranging Eq. 7, which provides Eq. 13. Combining the latter and Eq. 9 gives Eq. 14 to estimate the average cosine of α_i that is equivalent to the average orientation number in the direction *i*.

$$cos\,\alpha_i = \eta_i = \sqrt{\frac{\Delta L_i - k \cdot \gamma}{k \cdot (1 - \gamma)}} \qquad \textit{Eq. 13}$$

$$\eta_i = \sqrt{\frac{\Delta L_i \cdot (1 + 2 \cdot \gamma) - \Delta L \cdot \gamma}{\Delta L \cdot (1 - \gamma)}} \qquad \textit{Eq. 14}$$

Eq. 14 should be representative of the orientation number of a single fibre within the specimen or when all fibres are aligned in the same direction. If it is applied to a group of fibres dispersed with a certain randomness, this equation should provide an overestimation of the orientation number. The main reason for that is the bigger area available around the axis *i* with lower values of η_i. Consequently, there would be a higher probability of finding fibres with lower η_i, which is illustrated by Fig. 3.

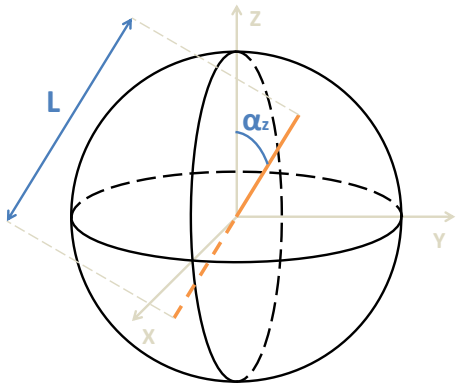

Fig. 3. Probabilistic distribution of fibres

In fact, assuming a perfectly isotropic medium with infinite fibres, the summed η_i for the three axes based on the inductive method could be calculated through Eq. 15. In this equation, cos α represents the relative inductive result of the fibres that form an angle α with the axis *i* and the sin α represents the surface available with this angle (see Fig. 3). Notice that the result of the summed integral in the three directions is 1.73.

$$\sum_{i=x,y,z} \eta_i = 3 \cdot \sqrt{\int_0^{90°} sin\,\alpha \cdot (cos\,\alpha)^2 \cdot d\alpha} = 1.73 \qquad \textit{Eq. 15}$$

For the same isotropic medium with infinite fibres, the real orientation number would be calculated according with Eq. 16, providing a summed result of 1.5. In reality, however, a certain anisotropy is usually present. Hence, values slightly smaller than 1.5 should be obtained. Such outcome is confirmed by the experimental results from other studies [34, 35] that show that the summed orientation number from three axes is between 1.4 and 1.5.

$$\sum_{i=x,y,z} \eta_i = 3 \cdot \int_0^{90^\circ} sin\,\alpha \cdot cos\,\alpha \cdot d\alpha = 1.5 \qquad \textit{Eq. 16}$$

In this case, it is evident that the direct application of Eq. 14 when non-aligned fibres are present would yield a total overestimation of approximately 0.3. Assuming that the variation is uniformly distributed, this is equivalent to an average overestimation of 0.1 for each axis. To account for that, a simple correction has to be applied to Eq. 14. In other words, the latter should be reduced by 0.1 in order to make it applicable when a considerably bigger number of fibres is present with a rather random distribution. Moreover, it is important to consider that in reality the magnetic field is not uniform inside the coil. Instead, it is subjected to small local distortions, as the fibres get closer to the extreme and the walls of the coil. Consequently, slightly smaller values of orientation number should be obtained. To correct this trend, Eq. 14 should be multiplied by a constant of approximately 1.03 valid for the test configuration proposed by Torrents et al. [28]

Applying both considerations described in the previous paragraph to Eq. 14 gives Eq. 16 that should be used in the assessment of the orientation number for the FRC. It is important to remark that a formulation to predict η_i was not available for the inductive method before. If properly validated, this formulation represents a contribution given the importance of η_i for the design of FRC structure. Moreover, it increases the amount of information that may be easily obtained with the test.

$$\eta_i = 1.03 \cdot \sqrt{\frac{\Delta L_i \cdot (1 + 2 \cdot \gamma) - \Delta L \cdot \gamma}{\Delta L \cdot (1 - \gamma)}} - 0.1 \qquad \textit{Eq. 16}$$

Eq. 16 also may be used to estimate the relative contribution of the fibres in a direction i (C_i). Following the same philosophy proposed by Torrents et al. [28], this relative contribution may be expressed through Eq. 17.

$$C_i = \frac{\eta_i}{\sum_{i=x,y,z} \eta_i} \qquad \textit{Eq. 17}$$

4. Experimental program

In total, two experimental programs were conducted. The first of them is dedicated to assess the accuracy and the repeatability of the method. The second is conducted to validate the formulations developed to assess the orientation number and the contribution of the fibres.

4.1. Accuracy of the method

4.1.1. Materials and methods

For the first experimental program, samples from 6 concrete mixes were tested with the inductive method and then crushed to assess the fibre content. To cover a wide range of materials, two types of concretes (conventional and self-compacting) with 3 fibre contents (30, 45 and 60 kg/m^3) were used. Table 1 presents the composition of the concrete mixes tested.

Table 1. Concrete mixes tested

Components	Characteristics	Content (kg/m³)					
		Conventional			Self-compacting		
Gravel (12/20 mm)	Granite	810			200		
Gravel (5/12 mm)	Granite	404			500		
Sand (0/5 mm)	Granite	817			1200		
Cement	CEM I 52,5 R	312			380		
Water	-	156			165		
Superplasticizer	Glenium TC 1425	2.19			4.56		
Hidratation activator	X SEED	6.24			7.6		
Fibres	Steel fibres	30	45	60	30	45	60
Reference		CC30	CC45	CC60	SC30	SC45	SC60
Slump (mm) according UNE 83503		3	5	3	-	-	-
Flow extent (mm) according EN 206		-	-	-	650	650	670

The steel fibres applied were BASF Masterfiber 502 with a circular cross-section, hooked ends, 50 mm of length and aspect-ratio equal to 50. These fibres are made of low carbon steel with approximately 3000 fibres per kg. A 250 litres vertical mixer was used to produce batches of 120 l. The fresh state properties measured are included in Table 1. In total, 4 cubic specimens with 150 mm were cast according with EN 12390-2 for each mix.

The set-up used for the inductive test follows strictly the defined in [28]. It was conducted with a pair of coils connected in parallel and separated 7.5 cm. The coil presents a square cross section with 17 cm of side, made with a copper cable of 0.2 mm of diameter and 1600 m of length (resulting in a total of 2354 turns). The inductance measurements were taken with the equipment AGILENT LCR 4263B. The equipment was set with an electrical alternating current, a frequency of 1 kHz and a voltage of 1 V.

The test procedure consisted of marking the three main axes of the cubic specimens. By default, the Z axis was parallel to the casting direction while the axes X and Y were parallel

to the sides of the moulds. Then the measurements were taken for the three directions. The same procedure is repeated several times in the same specimen in order to evaluate the repeatability of the method.

After that, the estimation of the fibre content was conducted following the standard EN 14721. The specimens were cracked with a hydraulic press and crushed in a grinding machine. Then, the fibres were separated with the help of a magnet and weighted. Considering the laborious and long time required, this procedure was performed only in 10 specimens: 5 of conventional and 5 of self-compacting concrete.

4.1.2. Results and analysis

Fig. 4.a shows the summed inductance (ΔL) measured and the content of fibres (C_f) weighted for the specimens. As expected, the results of the inductive method hold a linear relation with the content of fibre, displaying a high value of the coefficient of determination (R^2). This indicates the high accuracy of the inductive method in determining the fibre content. Moreover, the proportionality constant ω is equal to 0.4746 kg/m³·H for the fibre used.

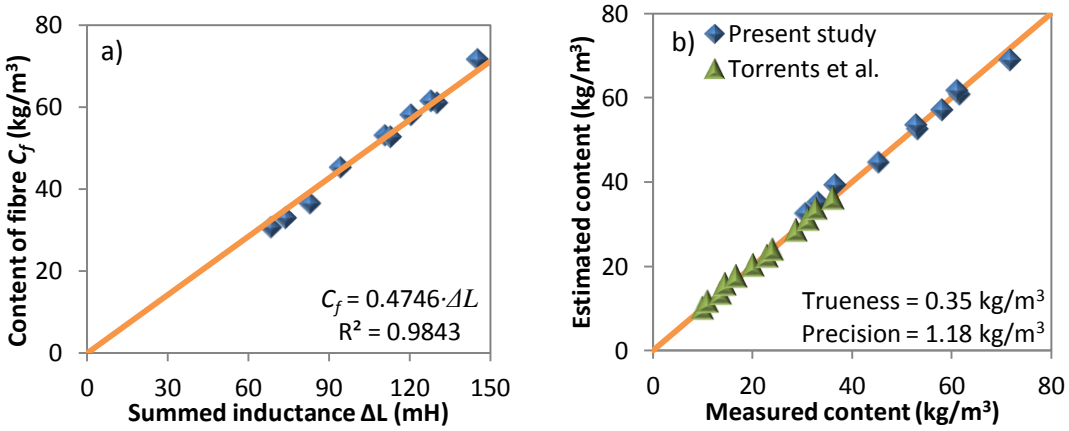

Fig. 4. Calibration curve (a) and accuracy of the method (b)

The fibre content estimated with the inductive method and the content measured by crushing the specimens (EN 14721:2008) is summarized in Fig. 4.b. The data obtained by Torrents et al. using the same experimental procedure as described here is also included to increase the size of the sample. The results obtained with the direct and the indirect measurement are similar for a wide range of fibre contents that vary from 10 kg/m³ to 70 kg/m³, approximately.

Although the fit is good in all cases, it is slightly better for the results of Torrents et al. [28]. This could be attributed to the use of concretes with significant differences in terms of consistency in the current experimental program. As expected, a much more anisotropic fibre distribution is observed in the SCC since the high flowability of the material favours the disposition of fibres perpendicular to the casting directions. This trend is less evident for the

CC in which, despite the effect of vibration, fibres tend to have more restrictions to their movement due to the low flowability of the material produced.

To quantify the accuracy of the inductive method in the estimation of the fibre content, the trueness and the precision is calculated with all data from Fig. 4.b according to the conceptual definition from the ISO 5725-1. For this assessment, the content measured by crushing is taken as a reference, even though a certain scatter might exist in this test. The small values obtained for trueness and precision show that the inductive method provides a good prediction of the fibre content with an average error of less than 2.12%.

Fig. 5 presents the relation between the result obtained with the inductive method in the first measurement and in the repetitions. This is presented for the inductance in each axis and for the estimation of the final content of fibres. The repeatability is calculated as the absolute difference between the first measurement and the repetition.

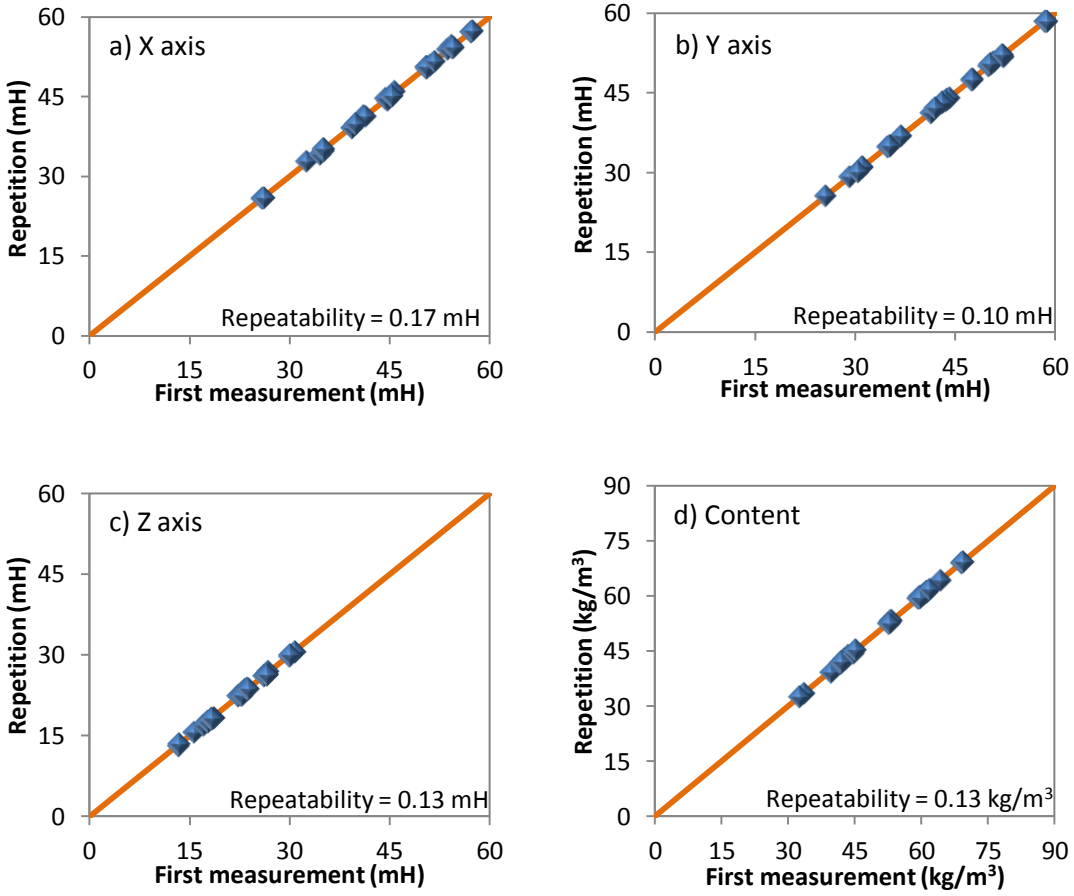

Fig. 5. Repeatability of the method

The results indicate that the test presents a good repeatability with relative errors that are on the average 0.40%, 0.22%, 0.58% and 0.27% of the measurements for X, Y, Z and the content, respectively. Notice that no clear relation was found between the casting direction and the magnitude of the error.

4.2. Experimental Validation of equations

4.2.1. Materials and methods

In order to validate the equations developed, cubic specimens were manufacture by gluing together several layers of non-magnetic cardboard sheets, as shown in Fig. 6. In some of the sheets, 150 g of the fibre used in the first experimental program were placed with the same alignment.

Fig. 6. Cardboard specimen with fibres

To simplify the production process, fibres uniformly distributed parallel to the XY plane at different heights (Z coordinates). The angle formed with the other faces of the cardboard specimen could vary. In total, specimens were produced with the angles of 0°, 10°, 20° and 30° with the X axis. Each of them was tested according with the same procedure described for the first experimental program. Since measurements were taken for the three main axes, the results are obtained for the angles of 0°, 10°, 20°, 30°, 60°, 70°, 80° and 90°.

4.2.2. Results and analysis

Fig. 7.a presents the orientation number estimated with Eq. 14 using the inductive results and the real values depending on the angle α_i between the fibres and the magnetic field. It is important to remark that Eq. 14 is used in this case given that the fibres are aligned. Notice that the real and the analytical curves practically overlap, showing almost the same results for the different angles assessed. The absolute error of estimation is smaller than $5 \cdot 10^{-3}$ on the average, which might be considered negligible.

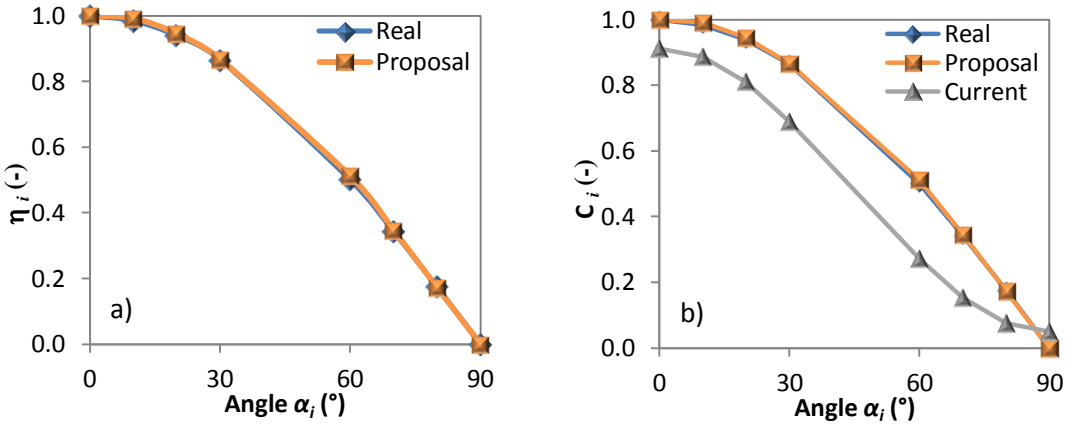

Fig. 7. Variation of the orientation number (a) and the fibre contribution (b) depending on the angle for the cardboard specimen

The contribution of fibre calculated with the experimental results in the current formulation from Torrents et al. (Eq. 2) and in the alternative proposal (Eq. 17) are presented in Fig. 7.b together with the real value from the cardboard specimen. It is evident that the current formulation provides an underestimation of the contribution of fibres for almost all angles considered. Besides, the shape of the estimated curve is completely different from the real one. In absolute terms, the error committed ranges from 0.05 up to 0.23, with relative values that go from 8.8% to 56.7%. In fact, with Eq. 2 it is impossible to achieve the contribution of 1 and of 0 as the angle formed approach 0° and 90°, respectively. This is due to the fact that the contribution of fibres orthogonal to the magnetic field is not considered in the formulation proposed by Torrents et al. [28].

On the contrary, the alternative formulation proposed here, not only is capable of reaching contributions of 0 and 1 for the extreme angles, but also approaches the real values with errors always smaller than 0.01. In relative terms, the errors are below 2.4% with an average of 0.68%. This confirms that the measurements obtained from the inductive method are proportional to the square of the cos α such as deducted in this paper, instead of proportional to the cos α such as indirectly assumed in Eq.2 from Torrents et al. [28].

5. Numerical Simulation

Even though the experimental program confirms the representativeness of the equation proposed for analysing the fibre contribution and orientation when an aligned configuration is present, it is still necessary to validate these formulations in case a rather random distribution of fibres exists. This situation is by far the most common in practice, being represented through Eq. 16 and 17.

In order to validate both equations for a wide range of anisotropic fibre distributions, a numerical analysis with finite elements is performed. This approach is select in opposition to an experimental verification since the latter would require a prohibitive number of real determinations of fibre orientation in specimens. Moreover, this is not considered necessary given the simple nature of the laws that govern the inductance change due to the presence of

fibres. Consequently, accurate predictions of the inductive test may be obtained with a properly validated finite element model (FEM).

5.1. Description of the FEM

With that in mind, a FEM composed by two modules was developed. The first modulus defines the distribution and the orientation of each fibre within a concrete specimen taking into account the wall effect of the formwork. The second modulus determines the inductance change produced in the coil when the inductive method is applied to this specimen. Finally, the real orientation and contribution of the FRC specimens is compared with the one predicted with Eq. 16 and 17 by using the inductance change. The following sections provide details about both modulus and the parametric study conducted with them.

5.1.1 Modulus 1: Distribution of the fibres

The disposition of each fibre in space is described by a vector $\vec{\mathrm{P}}$ taken from the origin of the coordinate system and a unitary vector $\vec{\mathrm{D}}$. The former defines the central point of the fibre whereas the latter defines its direction, as shown in Fig. 8. To determine the components of both vectors in the coordinate system axes, a probabilistic law is used.

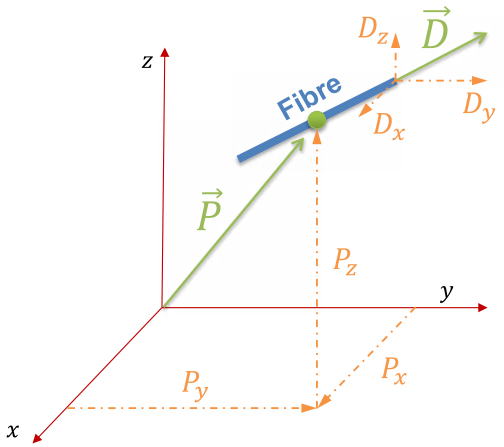

Fig. 8. Position and direction vectors of a fibre.

For a certain axis i, the position P_i is given by Eq. 18 in which ϕ is the cumulative Gauss distribution, V_{P_i} is a purely random variable generated between $V_{P_{i,max}}$ and $V_{P_{i,min}}$, μ_{P_i} is the average position of the fibre, σ_{P_i} is its standard deviation, whereas $P_{i,max}$ and $P_{i,min}$ indicate the limit position of the fibre in the space.

$$P_i = \frac{\phi\left(V_{P_i}, \mu_{P_i}, \sigma_{P_i}\right) \cdot \left(P_{i,max} - P_{i,min}\right)}{\phi\left(V_{P_{i,max}}, \mu_{P_i}, \sigma_{P_i}\right) - \phi\left(V_{P_{i,min}}, \mu_{P_i}, \sigma_{P_i}\right)} + P_{i,min} \qquad \textit{Eq. 18}$$

The same criteria is used to estimate $\vec{D}$. For that, first a transition vector Dt_i is determined according with Eq. 19. Then Dt_i is transformed into a unitary vector through Eq. 20. The variables used are analogous to the ones described for P_i. These equations allow a flexible representation of the fibre profile within the specimen. For example, if $V_{Dt_{i,min}} \approx V_{Dt_{i,max}}$, the distribution follow a uniform law. On the other hand, if $V_{Dt_{i,min}} \ll V_{Dt_{i,max}}$ it tends to a full Gauss distribution.

$$Dt_i = \frac{\phi\left(V_{Dt_i}, \mu_{Dt_i}, \sigma_{Dt_i}\right) \cdot \left(Dt_{i,max} - Dt_{i,min}\right)}{\phi\left(V_{Dt_{i,max}}, \mu_{D_i}, \sigma_{D_i}\right) - \phi\left(V_{Dt_{i,min}}, \mu_{Dt_i}, \sigma_{Dt_i}\right)} + Dt_{i,min} \qquad \textit{Eq. 19}$$

$$D_i = \frac{Dt_i}{\sqrt{{Dt_x}^2 + {Dt_y}^2 + {Dt_z}^2}} \qquad \textit{Eq. 20}$$

The influence of the walls of the formwork over the orientation of the fibres is a well-known phenomenon [36 - 38] also considered in the model. For that, an algorithm verifies if the extremities of the fibre falls outside the sampling area. If so, the probabilistic definition of the unitary vector $\vec{D}$ is repeated until the whole fibre is within the specimen. Fig. 9 shows a typical fibre distribution obtained for a cubic specimen with an approximately isotropic FRC.

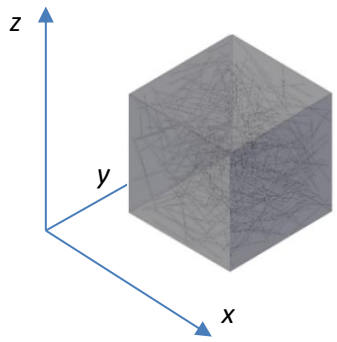

Fig. 9. Typical fibre distribution

5.1.2. Modulus 2: Estimation of inductance change

The estimation of the inductance change is performed with a FEM using a mesh formed by cubic brick elements with a side of 1 mm. The fibres were represented as straight lines discretized in 1 mm long stretches. The magnetic field is considered static since the wavelength produced by the electric current is much bigger than the dimensions of specimens or of the coil. In this case, the magnetic flux density (B) and the magnetic field (H) should follow Eq. 21 and 22, in which J represents the electric current density.

$$\nabla \cdot \vec{B} = 0 \qquad \textit{Eq. 21}$$

$$\nabla \, x \, \vec{H} = J \qquad \textit{Eq. 22}$$

Considering these and other classic equations from the electromagnetism theory, first the values of B and H are determined for every point of the mesh. Then, the averaged field is calculated for the central point of the different stretches of fibre inside the coil. Since the mutual inductance analogy should be valid, Eq. 3 is used to estimate the inductance change produced by each stretch along the length of the fibre. To account for the contribution perpendicular to its length, a shape factor (γ) is applied to the result. Finally, the summed inductance change produced by all fibres in a certain direction is obtained. This procedure is repeated for the main axes X, Y and Z in order to simulate the three measurements taken from each specimen. For this estimation, it is assumed that the magnetic permeability of the concrete and of the air may be considered approximately the same since both of them are several orders of magnitude smaller than that of the steel.

To illustrate the representativeness of the FEM, the experimental program described in 4.2 is simulated taking into account the approximate position of each fibre in space. Fig. 10 presents the inductance measured in the laboratory and the estimated with the FEM for the 4 specimens in X, Y and Z axes. It is evident that the FEM is capable of reproducing with a high accuracy the inductance change due to inclusion of fibres.

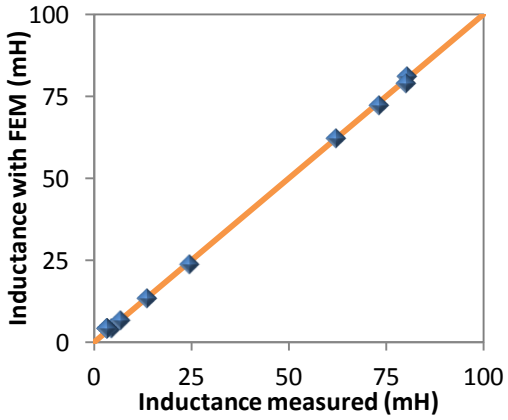

Fig. 10. Comparison between the real and the results of the FEM

5.1.2. Parametric study

A series of simulations were performed with the FEM using distribution profiles that are likely to be found in practice for the SFRC. It is known that the orientation of fibre is highly

affected by the casting and the vibration applied to the specimen during the production process as well as by the consistency of concrete. To account for variations that may occur in practice, different parameters are used in the modulus 1 responsible for the introduction of the fibres in the matrix.

The aim is to obtain SFRC specimens with different levels of anisotropy and to assess its influence in the accuracy of the analytical equation proposed in this study to estimate the orientation number (Eq. 16) and the contribution (Eq. 17) of fibres. This is performed by changing the values of the director vectors $V_{Dt_{i,min}}$ and $V_{Dt_{i,max}}$ for the main axes. Furthermore, to consider the use of fibres with different aspect ratios, simulations are performed with shape factors (γ) of 0.000, 0.025 and 0.050. A shape factor of 0 represent an ideal situation in which the cross section of the fibre tends to 0, whereas a shape factor of 0.05 is representative of the fibre used in the experimental program.

Table 2 summarizes all the combination of parameters analysed. In total, 63 different cases ranging from perfect isotropy to high anisotropy were analysed. For each case, 20 SFRC specimen were generated, always with a content of 60 kg/m³. Notice that, even though the input parameters are the same, a slightly different fibre distribution is obtained in each specimen due to the probabilistic laws involved in the distribution of the fibres. Consequently, the inductance measurements should present small variations among the specimens of the same case. In total 1260 analyses were performed.

Table 2. Parametric study

Cases	Director vectors						Shape Factor (γ)
	$V_{Dt_{x,min}}$	$V_{Dt_{y,min}}$	$V_{Dt_{z,min}}$	$V_{Dt_{x,max}}$	$V_{Dt_{y,max}}$	$V_{Dt_{z,max}}$	
1 to 3	-1	-1	-1	1	1	1	0.00, 0.025 and 0.050
4 to 6	-1	-1	-0.9	1	1	0.9	
7 to 9	-1	-1	-0.8	1	1	0.8	
10 to 12	-1	-1	-0.7	1	1	0.7	
13 to 15	-1	-1	-0.6	1	1	0.6	
16 to 18	-1	-1	-0.5	1	1	0.5	
19 to 21	-1	-0.9	-0.9	1	0.9	0.9	
22 to 24	-1	-0.9	-0.8	1	0.9	0.8	
25 to 27	-1	-0.9	-0.7	1	0.9	0.7	
28 to 30	-1	-0.9	-0.6	1	0.9	0.6	
31 to 33	-1	-0.9	-0.5	1	0.9	0.5	
34 to 36	-1	-0.8	-0.8	1	0.8	0.8	
37 to 39	-1	-0.8	-0.7	1	0.8	0.7	
40 to 42	-1	-0.8	-0.6	1	0.8	0.6	
43 to 45	-1	-0.8	-0.5	1	0.8	0.5	
46 to 48	-1	-0.7	-0.7	1	0.7	0.7	
49 to 51	-1	-0.7	-0.6	1	0.7	0.6	
52 to 54	-1	-0.7	-0.5	1	0.7	0.5	
55 to 57	-1	-0.6	-0.6	1	0.6	0.6	
58 to 60	-1	-0.6	-0.5	1	0.6	0.5	
61 to 63	-1	-0.5	-0.5	1	0.5	0.5	

5.2. Results and analysis

Fig. 11 relates the real orientation number calculated with the distribution of the fibres from the FEM and the orientation number estimated analytically with Eq. 16 based on the inductance change for the same specimen. The formulation developed provide accurate predictions with small errors. This is observed regardless of the aspect ratio of the fibre or the degree of anisotropy of the specimen. Based on the results, the trueness of the estimations with Eq. 16 is $7.25 \cdot 10^{-4}$ and the precision is $3.58 \cdot 10^{-3}$. In absolute terms, the average error of using the inductance measurements and the analytical proposal is of only 0.003, which is at least two orders of magnitude smaller than the usual values of η found in practice for each axis. In other words, the error of applying Eq. 16 to estimate η may be considered negligible.

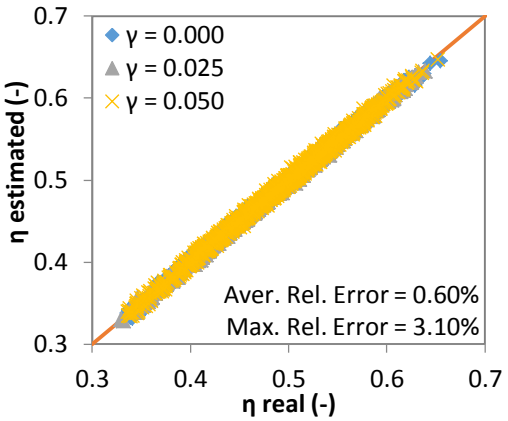

Fig. 11. Comparison between real and estimated orientation number

Fig. 12.a shows the comparison between the real contribution of the fibres in the specimens simulated and the contribution analytically estimated with the Eq. 2 proposed by Torrents et al. [28] based on the inductive change for the same specimen. A clear difference between both values is observed, especially as the contribution approaches extreme values that are characteristic of a high anisotropy. The average relative error expected in the prediction of the contribution of the fibres with Eq. 2 is of 5.67%, reaching a maximum of 24.33%.

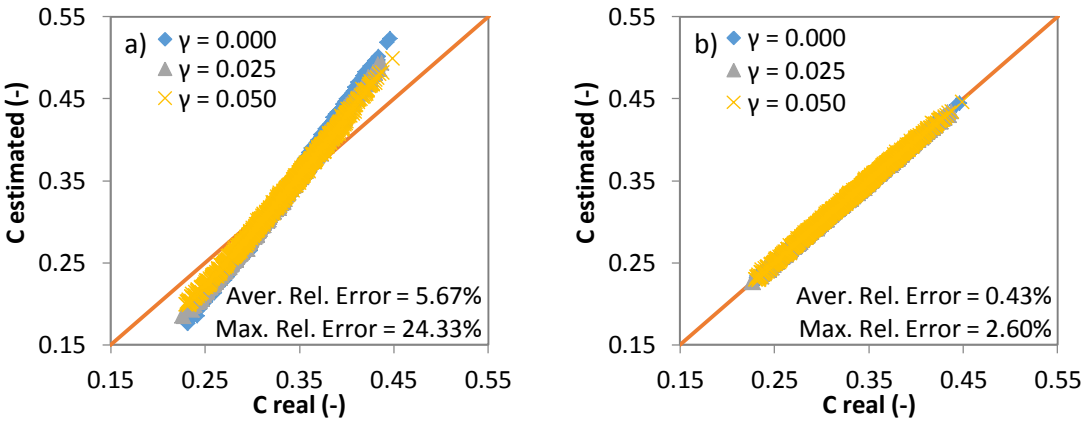

Fig. 12. Comparison between real contribution and contribution estimated with the original formulation (a) and with the alternative proposal (b)

The aspect ratio of the fibre represented through the shape factor also affects the error of estimation of the Eq. 2, which increases as the γ approaches 0. Nevertheless, for the range of parameters contemplated in this parametric study, the influence is much smaller than that of the level of the anisotropy of the specimen. For instance, the average relative error increases from 4.47% to 6.96% when the γ goes from 0.05 to 0. On the other hand, the introduction of anisotropy leads to an increase of more than 20% in the error of estimation of the real contribution of fibres based on the results of the inductive method.

The accuracy of the prediction of the fibre contribution with the alternative formulation (Eq. 17) is presented in Fig. 12.b. It shows that the values estimated analytically present a very good fit with the real contribution. In fact, the use of Eq. 17 yield a maximum and an average error of 2.60% and 0.43%, respectively. Notice that both errors are more than 10 times smaller than the calculated with the estimations from the Eq. 2 proposed by Torrents et al. [28]. This indicates a significant improvement achieved with Eq. 17 in terms of the prediction of the fibre contribution.

Such improvement also becomes evident when the influence of the shape factor on the estimation is analysed. Contrarily to the observed for the estimations with Eq. 2, the shape factor shows practically no influence in the error of the predictions with Eq. 17. For example, the average error for a shape factor of 0.000 and 0.050 are equal to 0.436% and 0.433%, respectively. It is evident that the new formulation proposed also represent an improvement on the representation of the physical phenomenon behind the inductive method.

7. Conclusions

In this study, several questions were raised regarding the application of the inductive method for the estimation of the fibre content and distribution in SFRC. After an extensive experimental and numerical study, the following conclusions may be derived.

- The analytical deductions performed indicate that the inductance change measured in the inductive test is proportional to the square of the cosine of the angle formed between the fibre and the reference axis. For this reason, the summed measurements at the three main axes should be linearly proportional to the fibre content. This explains why the inductive method is capable of predicting the fibre content once a calibration curve is obtained.

- The experimental program performed with different concrete types and fibre contents together with the data from the literature indicate that the method has a high accuracy. It is characterized by a trueness of 0.35 kg/m³, by a precision of 1.18 kg/m³ and by a repeatability of 0.13 kg/m³. These values may be considered adequate for the systematic quality control of FRC, thus supporting the use of the method.

- The experimental studies conducted indicate that the equations proposed by Torrents et al. provide an error of around 20% in the estimation of the fibre contribution in a certain direction. The FEM analysis performed with FRC specimens with a high level of

anisotropy corroborate such results. Instead, the Eq. 17 proposed in this study provide errors that are more than 10 times smaller in all verifications performed. Therefore, the latter should be used to predict the contribution of fibres in a certain direction.

- Formulations (Eq. 14 and 16) were deducted to predict the orientation number. The experimental and the numerical verification of the former indicate that they are capable of predicting the orientation number based on the results of the inductive method. The studies conducted show that the average error of prediction should be below 0.50%. The formulations proposed make it possible to obtain an important parameter that could not be assessed before with the inductive method. This opens up a new field of application for the test.

Acknowledgements

The authors thank the collaboration of Pau Juan during the experimental an theoretical developments included in this work.

Referencias

[1] Mobasher B, Stang H, Shah SP. Microcracking in fiber reinforced concrete. Cem Concr Res 1990;20(5): 665-76.

[2] Bentur A. Fiber-reinforced cementitious materials. Mater Scien Concr 1989: 223-85.

[3] Blanco A. Characterization and modelling of SFRC elements. PhD Thesis, Universitat Politècnica de Catalunya 2013.

[4] Van Gysel A. Studie van het uittrekgedrag van staalvezels ingebed in een cementgebonden matrix met toepassing op staalvezelbeton onderworpen aan buiging. PhD thesis. University of Ghent 2000.

[5] Lange-Kornbak D, Karihaloo BL. Design of fiber-reinforced DSP mixes for minimum brittleness. Advanced Cem based Mater 1998;7(3): 89-101.

[6] Li VC. Postcrack scaling relations for fiber reinforced cementitious composites. J Mater Civ Eng, ASCE 1992;4(1):41-57.

[7] Brandt AM. On the optimal direction of short metal fibres in brittle matrix composites. J Mater Scien 1985;20(11):3831-41.

[8] Ferrara L, Meda A. Relationships between fibre distribution, workability and the mechanical properties of SFRC applied to precast roof elements. Mater Struct 2006;39(4):411-20.

[9] Deutsche Beton Vereins. DBV Merkblatt Stahlfaserbeton. Deutscher Beton-Und Bautechnik-Verein 2001.

[10] RILEM TC 162-TDF. Test and design methods for steel fibre reinforced concrete - σ-ε design method: Final Recommendation. Mater Struct 2003;36(262):560-67.

[11] CNR-DT 204. Istruzioni per la Progettazione, l'Esecuzione ed il Controllo di Strutture Fibrorinforzato. Consiglio Nazionale delle Riserche, Italia 2006.

[12] CEB-FIP. Model Code. Comité Euro-International du Beton-Federation International de la Precontraint, Paris 2010.

[13] Comisión permanente del Hormigón. Instrucción del Hormigón Estructural, EHE-08. Anejo 14. Ministerio de Fomento, gobierno de España 2008.

[14] Robins PJ, Austin SA, Jones PA. Spatial distribution of steel fibres in sprayed and cast concrete. Mag Concr Res 2003;55(3):225-35.

[15] Vandewalle L, Heirman G, van Rickstal F. Fibre orientation in self-compacting fibre reinforced concrete. In: Proceedings of the 7th RILEM symposium on fibre reinforced concrete: design and applications (BEFIB 2008) 2008, Chennai, India, pp 719–728.

[16] Van Gysel A. Studie van het uittrekgedrag van staalvezels ingebed in een cementgebonden matrix met toepassing op staalvezelbeton onderworpen aan buiging. PhD Thesis. Gent University 2000.

[17] Molins C, Martinez J, Arnáiz N. Distribución de fibras de acero en probetas prismáticas de hormigón. In: CD-ROM from the 4th international structural concrete congress (ACHE) 2008, Valencia, Spain.

[18] Schnell J, Ackermann FP, Rösch R, Sych T. Statistical analysis of the fibre distribution in ultra high performance concrete using computer tomography. In Proceedings of the Second International Symposium on UHPC 2008, Kassel, Germany (pp. 145-152).

[19] Redon C, Chermant L, Chermant JL, Coster M. Assessment of fibre orientation in reinforced concrete using Fourier image transform. J Microscopy 1998;191:258-65.

[20] Ozyurt N, Mason TO, Shah SP. Non-destructive monitoring of fiber orientation using AC-IS: An industrial-scale application. Cem Concr Res 2006;36(9):1653-60.

[21] Ozyurt N, Woo LY, Mason TO, Shah SP. Monitoring fiber dispersion in fiber-reinforced cementitious materials: comparison of AC impedance spectroscopy and image analysis. ACI Mater J 2006, 103(5).

[22] Torrents JM, Juan-García P, Patau O, Aguado A. Surveillance of steel fibre reinforced concrete slabs measured with an open-ended coaxial probe. In: Proceedings of the XIX IMEKO world congress: fundamental and applied metrology 2009, Lisbon, Portugal, pp 2282–84. http://www.imeko2009.it.pt/Papers/FP_633.pdf. Accessed 5 Jan 2012

[23] Van Damme S, Franchois A, De Zutter D, Taerwe L. Nondestructive determination of the steel fiber content in concrete slabs with an open-ended coaxial probe. IEEE Trans Geosci Remote Sens 2004;42(11):2511-21.

[24] Lataste JF, Behloul M, Breysse D. Characterisation of fibres distribution in a steel fibre reinforced concrete with electrical resistivity measurements. NDT & E Int 2008;41(8):638-47.

[25] Barnett SJ, Lataste JF, Parry T, Millard SG, Soutsos MN. Assessment of fibre orientation in ultra high performance fibre reinforced concrete and its effect on flexural strength. Mater Struct 2010;43(7):1009-23.

[26] Faifer M, Ottoboni R, Toscani S, Ferrara L. Steel fiber reinforced concrete characterization based on a magnetic probe, Instrumentation and Measurement Technology Conference (I2MTC) 2010, IEEE: 157–62.

[27] Faifer M, Ferrara L, Ottoboni R, Toscani S. Low Frequency Electrical and Magnetic Methods for Non-Destructive Analysis of Fiber Dispersion in Fiber Reinforced Cementitious Composites: An Overview. Sensors 2013;13(1):1300-18.

[28] Torrents JM, Blanco A, Pujadas P, Aguado A, Juan-García P,Sánchez-Moragues MÁ. Inductive method for assessing the amount and orientation of steel fibers in concrete. Mater Struct 2012;45(10):1577-92.

[29] Molins C, Aguado A, Saludes S. Double punch test to control the energy dissipation in tension of FRC (Barcelona test). Mater Struct 2009;42(4),415-25.

[30] Laranjeira F, Grünewald S, Walraven J, Blom C, Molins C, Aguado A. Characterization of the orientation profile of steel fiber reinforced concrete. Mater Struct 2011;44(6):1093-111.

[31] Laranjeira F, Aguado A, Molins C, Grünewald S, Walraven J, Cavalaro, S. Framework to predict the orientation of fibers in FRC: a novel philosophy. Cem Concr Res 2012;42(6),752-68.

[32] Grünewald, S. (2004). Performance-based design of self-compacting fibre reinforced concrete. PhD Thesis, Delft University of Technology.

[33] Schönlin K. Ermittlung der Orientierung, Menge und Verteilung der Fasern in faserbewehrtem Beton. Beton-und Stahlbetonbau 1988;83(6):168-71.

[34] Laranjeira F.Design-oriented constitutive model for steel fiber reinforced concrete. PhD Thesis, Universitat Politècnica de Catalunya 2010.

[35] Dupont D, Vandewalle L. Distribution of steel fibres in rectangular sections. Cem Concr Compos 2005;27(3):391-8.

[36] Soroushian P, Lee CD. Distribution and orientation of fibers in steel fiber reinforced concrete. ACI Mater J 1990;87(5).

[37] Kameswara Rao CVS. Effectiveness of random fibres in composites. Cem Concr Res 1979;9(6):685-93.

[38] Martinie L, Roussel N. Simple tools for fiber orientation prediction in industrial practice. Cem Concre Res 2011;41(10):993-1000.

Dear Editor,

We are pleased to submit our original research paper entitled "IMPROVED ASSESSMENT OF FIBRE CONTENT AND ORIENTATION WITH INDUCTIVE METHOD IN SFRC" to Materials and Structures. This study has a starting point in a previous paper published in the same journal by Torrents et al. (2009) about the use of the inductive method to assess the fibre content and distribution in SFRC. Despite the advantages in comparison with other methods, further studies are still needed to define the accuracy, the theoretical basis of the test and the equations for the conversion of the inductance measurements into fibre content and distribution. The analysis performed here indicates that the equations proposed by Torrents et al. (2009) may lead to errors of up to 24% in case of SFRC with high anisotropy. Another drawback of the method is that no equation exists for the estimation of the orientation number, which is a valuable parameter for the design of structures.

The objective of the present paper is to address this issue. Initially, the theoretical basis for the calculation of the fibre content is provided. Then, alternative equations are deducted for the fibre contribution and for the orientation number. Different experimental programs and finite element numerical simulations are conducted to evaluate the accuracy of the method and to validate the proposals. The results shows that the formulation proposed here show errors far below 2.6%, allowing the prediction of the orientation number in all directions with high accuracy. This opens up a new field of application for the test and represents an advance towards the characterization and the quality control of SFRC.

We hope that the content of the paper and the study conducted fit the scope of the journal. We put ourselves entirely at your service to perform any changes or improvements you consider necessary.

Sincerely yours,

Sergio H. P. Cavalaro
Rubén López
Josep María Torrents
Antonio Aguado

Fig. 1
Click here to download colour figure: Figure 1.docx

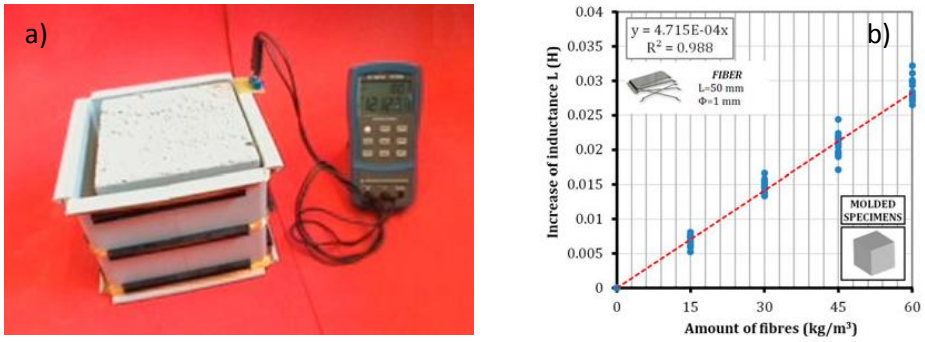

Fig. 1.- Inductive method proposed by Torrents et al. [28] (a) and typical relation between inductance change and fibre content (b)

Fig. 2
Click here to download colour figure: Figure 2.docx

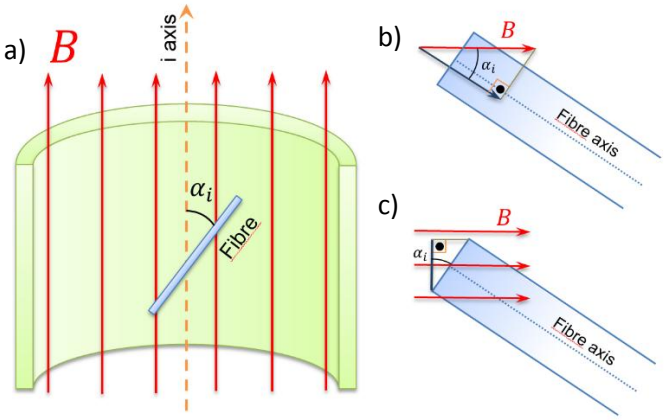

Fig. 2. Single fibre inside a coil (a) and decomposition of the magnetic flux through the fibre (b and c)

Fig. 3
Click here to download colour figure: Figure 3.docx

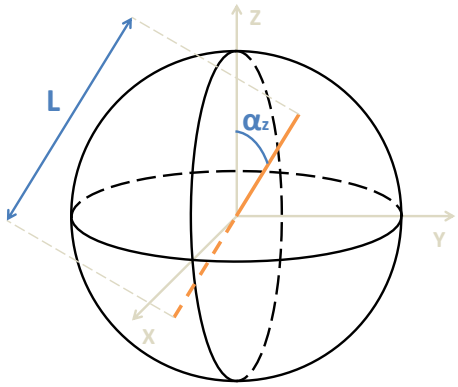

Fig. 3. Probabilistic distribution of fibres

Fig. 4
Click here to download colour figure: Figure 4.docx

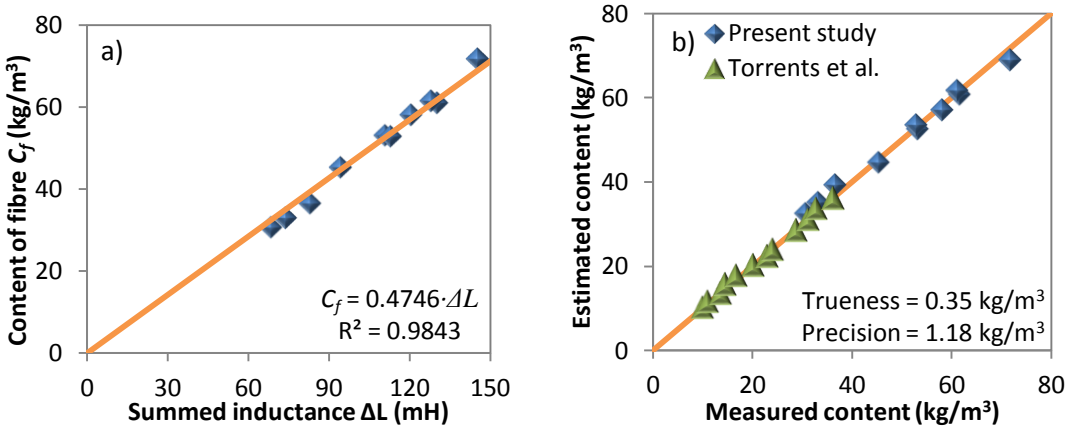

Fig. 4. Calibration curve (a) and accuracy of the method (b)

Fig. 5
Click here to download colour figure: Figure 5.docx

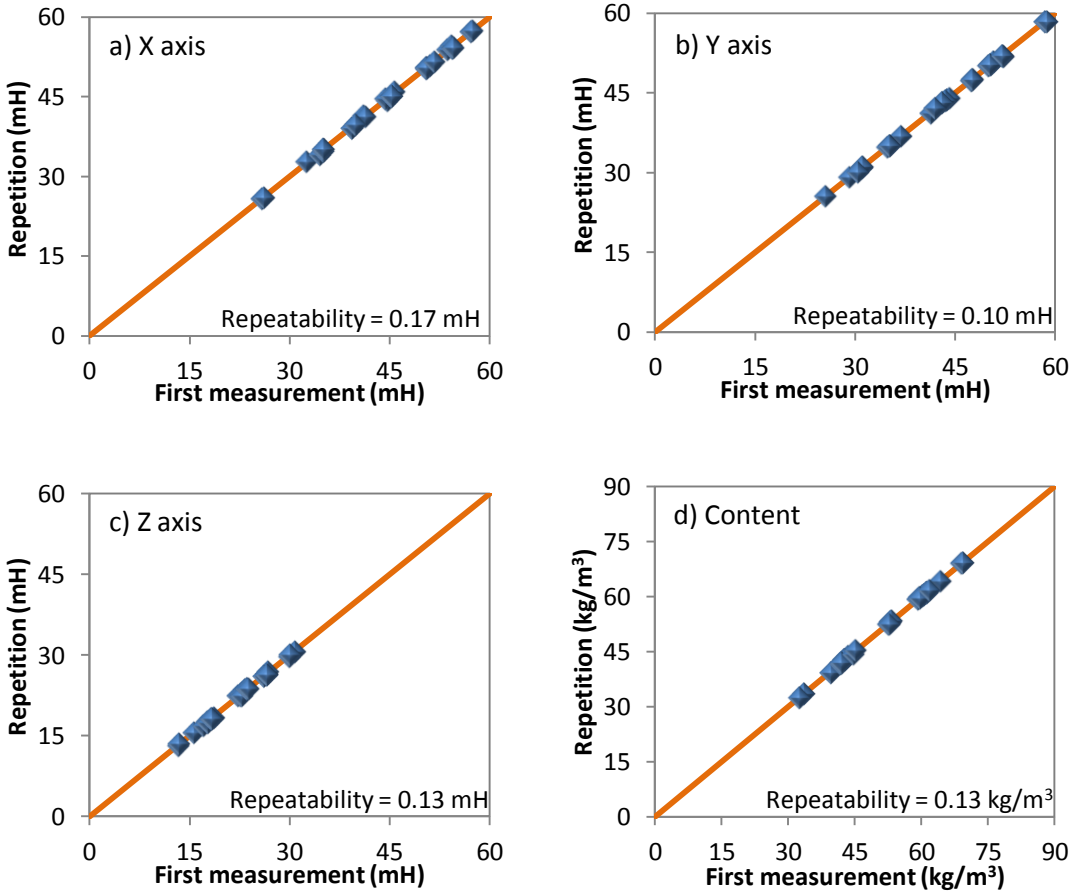

Fig. 5. Repeatability of the method

Fig. 6
Click here to download colour figure: Figure 6.docx

Fig. 6. Cardboard specimen with fibres

Fig. 7
Click here to download colour figure: Figure 7.docx

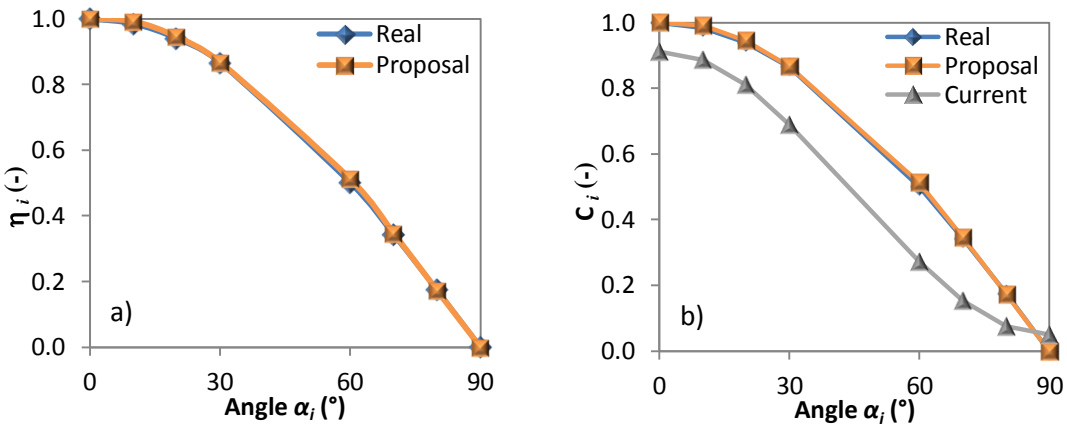

Fig. 7. Variation of the orientation number (a) and the fibre contribution (b) depending on the angle for the cardboard specimen

Fig. 8
Click here to download colour figure: Figure 8.docx

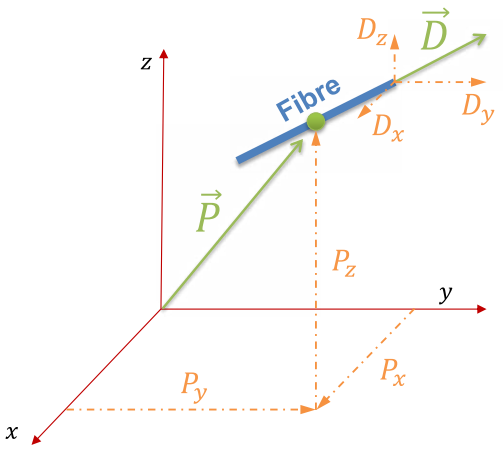

Fig. 8. Position and direction vectors of a fibre.

Fig. 9
Click here to download colour figure: Figure 9.docx

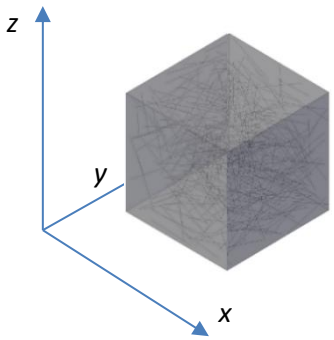

Fig. 9. Typical fibre distribution

Fig. 10
Click here to download colour figure: Figure 10.docx

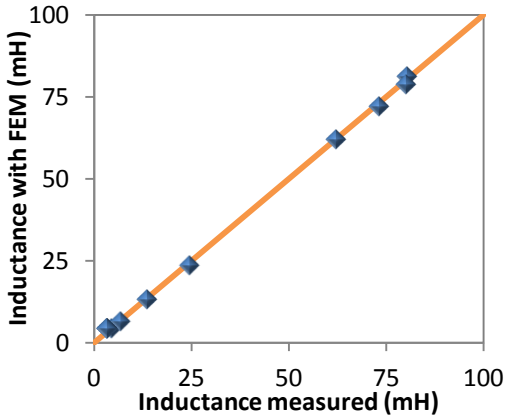

Fig. 10. Comparison between the real and the results of the FEM

Fig. 11
Click here to download colour figure: Figure 11.docx

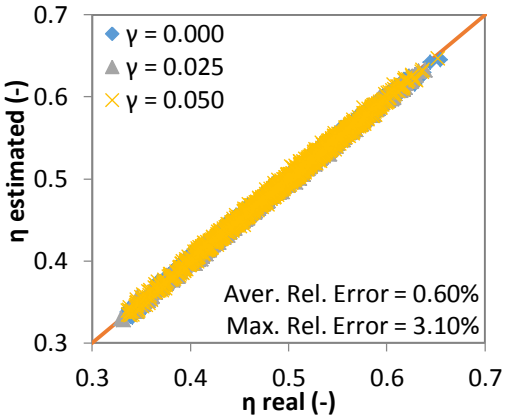

Fig. 11. Comparison between real and estimated orientation number

Fig. 12
Click here to download colour figure: Figure 12.docx

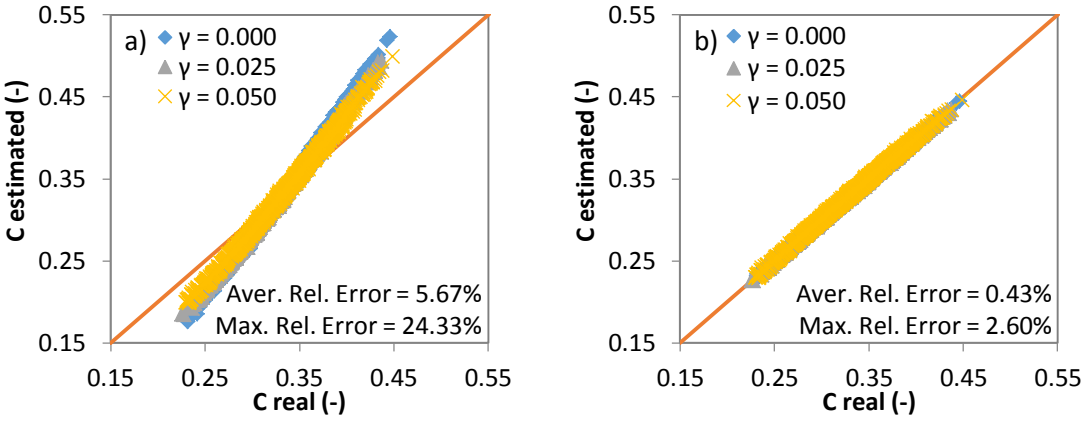

Fig. 12. Comparison between real contribution and contribution estimated with the original formulation (a) and with the alternative proposal (b)

Table 1
Click here to download table: Table 1.docx

Table 1. Concrete mixes tested

Components	Characteristics	Content (kg/m³)					
		Conventional			Self-compacting		
Gravel (12/20 mm)	Granite	810			200		
Gravel (5/12 mm)	Granite	404			500		
Sand (0/5 mm)	Granite	817			1200		
Cement	CEM I 52,5 R	312			380		
Water	-	156			165		
Superplasticizer	Glenium TC 1425	2.19			4.56		
Hidratation activator	X SEED	6.24			7.6		
Fibres	Steel fibres	30	45	60	30	45	60
Reference		CC30	CC45	CC60	SC30	SC45	SC60
Slump (mm) according UNE 83503		3	5	3	-	-	-
Flow extent (mm) according EN 206		-	-	-	650	650	670

Table 2
Click here to download table: Table 2.docx

Table 2. Parametric study

Cases	Director vectors						Shape Factor (γ)
	$V_{Dt_{x,min}}$	$V_{Dt_{y,min}}$	$V_{Dt_{z,min}}$	$V_{Dt_{x,max}}$	$V_{Dt_{y,max}}$	$V_{Dt_{z,max}}$	
1 to 3	-1	-1	-1	1	1	1	0.00, 0.025 and 0.050
4 to 6	-1	-1	-0.9	1	1	0.9	
7 to 9	-1	-1	-0.8	1	1	0.8	
10 to 12	-1	-1	-0.7	1	1	0.7	
13 to 15	-1	-1	-0.6	1	1	0.6	
16 to 18	-1	-1	-0.5	1	1	0.5	
19 to 21	-1	-0.9	-0.9	1	0.9	0.9	
22 to 24	-1	-0.9	-0.8	1	0.9	0.8	
25 to 27	-1	-0.9	-0.7	1	0.9	0.7	
28 to 30	-1	-0.9	-0.6	1	0.9	0.6	
31 to 33	-1	-0.9	-0.5	1	0.9	0.5	
34 to 36	-1	-0.8	-0.8	1	0.8	0.8	
37 to 39	-1	-0.8	-0.7	1	0.8	0.7	
40 to 42	-1	-0.8	-0.6	1	0.8	0.6	
43 to 45	-1	-0.8	-0.5	1	0.8	0.5	
46 to 48	-1	-0.7	-0.7	1	0.7	0.7	
49 to 51	-1	-0.7	-0.6	1	0.7	0.6	
52 to 54	-1	-0.7	-0.5	1	0.7	0.5	
55 to 57	-1	-0.6	-0.6	1	0.6	0.6	
58 to 60	-1	-0.6	-0.5	1	0.6	0.5	
61 to 63	-1	-0.5	-0.5	1	0.5	0.5	